# Possible crystal-field excitation in single-crystal CeNiSn

J.-G. Park
*Department of Physics, Inha University, Inchon 402-751, Korea*

D. T. Adroja
*Department of Physics, Southampton University, Southampton SO17 1BJ, United Kingdom*

K. A. McEwen*
*Department of Physics, Birkbeck College, University of London, London WC1E 7HX, United Kingdom*

Y. J. Bi
*School of Metallurgy and Materials, Faculty of Engineering, University of Birmingham, Birmingham B15 2TT, United Kingdom*

J. Kulda
*Institut Laue-Langevin, 38042 Grenoble Cedex 9, France*
(Received 11 August 1997; revised manuscript received 21 April 1998)

We present inelastic-neutron-scattering results for single-crystal CeNiSn. Apart from phonon-related structures appearing mainly below 30 meV, we have observed clear indications of a crystal-field excitation centered around 40 meV. However, we cannot yet determine whether there is another crystal-field excitation at a lower energy because of the presence of strong phonon peaks. We have also made measurements to investigate the quasielastic response of CeNiSn. We discuss the current understanding of CeNiSn with reference to our findings. [S0163-1829(98)08829-8]

## I. INTRODUCTION

CeNiSn is a strongly correlated electron system which shows an interesting low-temperature behavior, namely a low carrier Kondo-like behavior.[1] Its heat capacity is reduced remarkably below 10 K, thus implying that its density of states is suppressed at low temperatures. On the other hand, $^{119}$Sn NMR spectra at low temperatures have been interpreted in terms of a V-shaped gap opening at the Fermi level.[2] Hall coefficient measurements also show that the number of conduction electrons decreases at low temperatures.[3] However, it has been found recently that the sharp increase in resistivity at low temperatures which was originally taken as a signature of the development of a gap is in fact very sensitive to small impurities present in samples. Surprisingly enough, CeNiSn samples with better quality have a less pronounced low-temperature upturn and furthermore samples of the best quality become metallic at lower temperatures.[4] In fact, the early indication of the low-temperature metallic regime was noted by Mason *et al.*[5] It is also interesting to note that unlike the sample-dependent resistivity upturn, the electronic specific heat extrapolated to $T=0$ K; $\gamma=60$ mJ/mol K$^2$, does not depend on sample quality. Together with the resistivity behavior, this indicates that despite the small gap opened in the density of charge carriers there is nevertheless some residual density of states left inside the gap.

As well as the results discussed above, the inelastic-neutron-scattering data are also particularly interesting. Below the coherence temperature of 20 K, where every hybridized $f$ electron is expected to form a Bloch state, there appear two magnetic excitations which are strongly localized in reciprocal space; one at 2 meV and the other at 4 meV.[5] That they appear at low temperatures seems to indicate that they originate from a coherent Kondo state. However, despite the interesting features of the low-energy magnetic excitations in CeNiSn, the question of crystal-field excitations in CeNiSn is not yet well understood. Moreover, it was proposed by one group that the low-lying gaplike excitations seen in neutron scattering, together with other low-temperature features of the bulk measurements, are due to strong hybridization between crystal-field excitations of very low energy (less than the Kondo temperature of 80 K) and the conduction band.[6] In this respect, it is very interesting to note that according to recent neutron studies of polycrystalline Ce(Pt,Ni)Sn, two well-defined crystal-field excitations found in CePtSn, a localized Ce system, become weaker with Ni doping.[7] It is particularly important that these excitations changed very smoothly and appeared to be present even in pure CeNiSn. If the polycrystal data are indeed correct, then they have very significant implications for the understanding of the low-lying excitations at 2 and 4 meV, and also of the low-temperature features of the bulk measurements.

In order to confirm the presence of crystal-field excitations seen in polycrystal CeNiSn, we decided to investigate the inelastic neutron scattering from a single crystal of CeNiSn. Here we present results of the crystal-field excitations of CeNiSn using a well characterized single crystal.

## II. EXPERIMENTAL DETAILS

A single crystal of CeNiSn was grown, at the University of Birmingham, by the Czochralski method using a tungsten crucible under an atmosphere of purified Ar at 2 bars. The pulling rate was 28 mm/h. The initial charge of CeNiSn with a stoichiometric composition was prepared by arc melting from high-purity starting materials. Laue x-ray diffraction showed that the as-grown boule was a good single crystal. A $b$-axis cylindrical shaped sample of mass 7 g was cut out for the neutron-scattering experiments.

Inelastic-neutron-scattering measurements were carried out using the IN8 thermal neutron triple-axis spectrometer at the Institut Laue-Langevin, Grenoble. The collimation was 50′-40′-open-open. With the vertically focusing Cu(111) monochromator and the horizontally focusing PG (002) analyzer crystals, we operated at fixed $k_F = 4.1$ Å$^{-1}$. This configuration gave us a maximum energy transfer of 64 meV with a typical energy resolution of 3 meV for zero energy transfer and of 4–5 meV at 30 meV energy transfer. The background signal was measured for a typical scan by aligning the analyzer 3° away from the Bragg reflecting position. From these results, we could ensure that the background was very low over the energy range of interest. This will be presented together with the other data for comparison. For quasielastic measurements we used PG (002) monochromator and elastically bent Si(111) analyzer crystals, giving better resolution at low energy transfer. The resolution of the low-energy setup is 0.7 meV at elastic energy. We used an ILL standard Orange cryostat for the low-temperature measurements. Most of our measurements were made at 2 K, but we also measured a scan at 25 K for comparison. The sample was mounted with its $b^*$ and $c^*$ axes in the horizontal scattering plane.

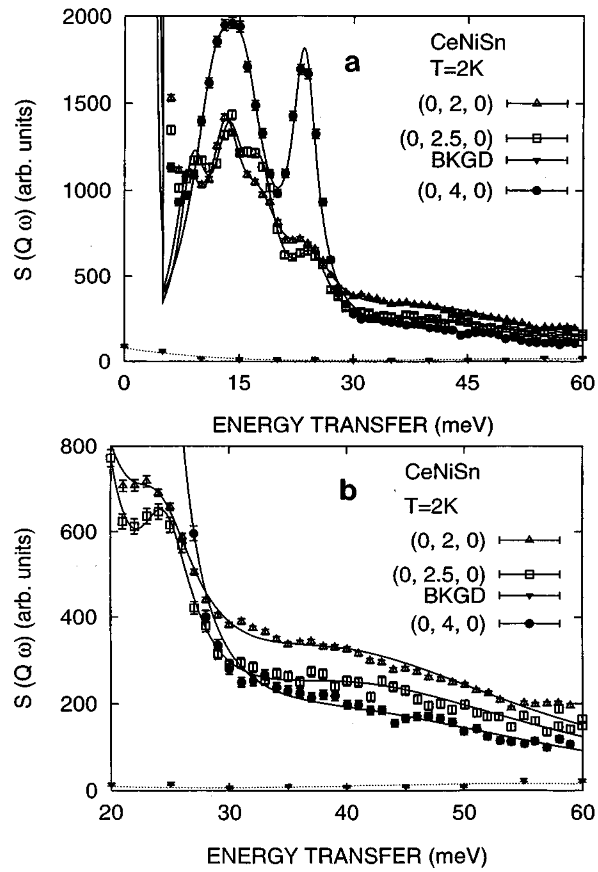


FIG. 1. (a) Inelastic-neutron-scattering spectra for $Q=(0,k,0)$, with $k=2$, 2.5, and 4. The solid lines are fits to the experimental data with Lorentzian functions using the parameters given in Table I. The dashed line is the background at $Q=(0,2.5,0)$ measured as described in the text. The high-energy results are shown enlarged in (b).

## III. RESULTS AND ANALYSIS

### A. (0,*k*,0) scans

The results of energy transfer scans at $Q=(0,2,0)$, (0,2.5,0), and (0,4,0) are shown in Fig. 1(a). As can be seen, several intense peaks are apparent below 30 meV; altogether there are four peaks centered at 8, 13, 17, and 24 meV, and an additional broad feature appears centered at around 40 meV. The peak at 8 meV was seen at almost the same energy in (0,2,0) and (0,2.5,0) scans, but is completely absent in (0,4,0) scans. This peak was not seen in any other scans we studied, for example, in the $(0,0,l)$ and $(0,k,k)$ scans. It is rather surprising that the center of this peak does not move as $Q$ changes from zone center to zone boundary, and then it disappears in all the other scans in reciprocal space that we measured.

The 40-meV structure is more clearly observable in Fig. 1(b), which shows the high-energy data in detail. The background signal for the (0,2.5,0) scan with the analyzer offset is also presented in Fig. 1. Regarding the $Q$ dependence of the peaks, it is noticeable that the 40-meV structure becomes weaker with increasing $Q$ while the peaks below 30 meV increase significantly for $Q$ values between (0,2,0) and (0,4,0) (see Fig. 1). However, the low-energy part of the (0,2.5,0) scan does not follow this pattern: the peak at 24 meV remains almost the same in the (0,2.5,0) scan. Except for the 24-meV peak in the (0,2.5,0) scan, the peaks below 30 meV grow with increasing wave vector whereas the 40-meV peak behaves otherwise. This different $Q$ dependence suggests that the low-energy peaks arise from phonon excitations, but the 40-meV peak is likely to be due to a magnetic excitation. We recall that the phonon cross section increases as $Q^2$ while the magnetic cross section decreases with increasing $Q$ as $[f(Q)]^2$, where $f(Q)$ is the $Ce^{3+}$ magnetic form factor. This confirms that the excitations centered at 40 meV have a magnetic nature, while those below 30 meV are primarily due to phonons. Then we may be able to understand the $Q$ dependence of the intensity of the 24 meV in the (0,2.5,0) scan in terms of a smaller phonon structure factor at the zone boundary. Within experimental error, we could not observe any temperature dependence of the (0,2,0) scan between 2 and 25 K.

Unlike the phonon peaks, the 40-meV structure is very broad; for example in the (0,2,0) scan the linewidth is about 19 meV for the 40-meV excitation and less than 5 meV for the phonon peaks (see Table I). The linewidths in Table I are half-width at half-maximum values. The very broad nature of the 40-meV excitation indicates that the $4f$ electrons in CeNiSn are strongly hybridized with the conduction electrons. However, this hybridization is not strong enough to destroy the magnetic excitations completely as in some heavy fermion compounds such as $CeCu_6$ and in Ce mixed valence systems.[8] We will discuss this point later when we examine the ground state of CeNiSn. Table I summarizes the results of fitting a set of Lorentzian functions to our experimental data.

TABLE I. Summary of curve fitting results.

| | (0,2,0) | (0,2.5,0) | (0,4,0) | (0,0,3.2) | (0,0,4) | (0,0,6) | (0,2,2) | (0,4,4) |
|---|---|---|---|---|---|---|---|---|
| Peak 1 Center (meV) | 39.7 | 40.7 | 41.2 | 39.1 | 39.7 | 38.5 | 36.9 | 36.9 |
| Linewidth (meV) | 19.0 | 19.0 | 19.0 | 19.0 | 19.6 | 18.6 | 20.4 | 20.4 |
| Area (a.u.) | 228 | 171 | 104 | 240 | 204 | 129 | 239 | 108 |
| Peak 2 Center (meV) | 24.0 | 24.5 | 23.6 | 24.5 | 23.9 | 23.5 | 24.6 | 24.5 |
| Linewidth (meV) | 4.0 | 2.9 | 2.0 | 2.4 | 2.4 | 2.8 | 2.4 | 2.2 |
| Area (a.u.) | 113 | 88 | 247 | 96 | 76 | 93 | 77 | 67 |
| Peak 3 Center (meV) | 17.6 | 17.8 | 15.5 | | | | 15.9 | 18.1 |
| Linewidth (meV) | 3.6 | 2.5 | 3.5 | | | | 2.5 | 1.5 |
| Area (a.u.) | 214 | 207 | 471 | | | | 153 | 100 |
| Peak 4 Center (meV) | 13.1 | 13.6 | 11.8 | 12.0 | 13.0 | 12.9 | 11.3 | 13.0 |
| Linewidth (meV) | 2.6 | 2.6 | 3.8 | 6.0 | 5.2 | 3.1 | 5.0 | 3.8 |
| Area (a.u.) | 372 | 357 | 749 | 922 | 1077 | 1448 | 872 | 2046 |
| Peak 5 Center (meV) | 8.2 | 8.9 | | | | | | |
| Linewidth (meV) | 2.2 | 2.2 | | | | | | |
| Area (a.u.) | 390 | 416 | | | | | | |

### B. (0,0,*l*) scans

Figures 2(a) and 2(b) show results for energy transfer scans for $l=3.2$, 4, and 6 together with the fitted curves. The peak seen around 17 meV in the (0,*k*,0) scans is absent in all the (0,0,*l*) scans (see Fig. 2 and Table I). For the (0,*k*,0) scans, we found that the 17-meV peak moves towards lower energy transfer with increasing $Q$ from (0,2,0) to (0,4,0). On the other hand, the 40-meV structure becomes weaker with increasing $Q$ in the (0,0,*l*) scans as in the (0,*k*,0) scans. However, the center of the peak hardly changes from (0,0,3.2) to (0,0,6) (see Table I): it remains at almost the same energy within the instrumental resolution. As noted in Sec. III A, the 8 meV is absent in all the (0,0,*l*) scans.

### C. (0,*k*,*k*) scans

Figure 3 shows the data for $Q=(0,2,2)$ and (0,4,4) scans. Like the previous spectra for the (0,*k*,0) and (0,0,*l*) scans, the 40-meV peak becomes weaker with increasing $Q$. It is rather surprising to see that the intensity of the 24-meV peak is reduced with $Q$ (see Table I). In the (0,*k*,0) and (0,0,*l*) scans, it always grows with increasing $Q$ when compared with all the zone-center data. It may possibly be due to different phonon structure factors for (0,2,2) and (0,4,4). The middle phonon peak, which was seen at 17.6 meV for (0,2,0), appears at 15.9 meV for (0,2,2), and moves to 18.1 meV for (0,4,4) and at the same time is reduced in intensity. We note that the intensities of the 13-meV peak more than double from (0,2,2) to (0,4,4).

### D. Quasielastic peak scans

We also made measurements of the quasielastic peak at $Q=(0,0,3.5)$ between 2 and 160 K to investigate the tem-

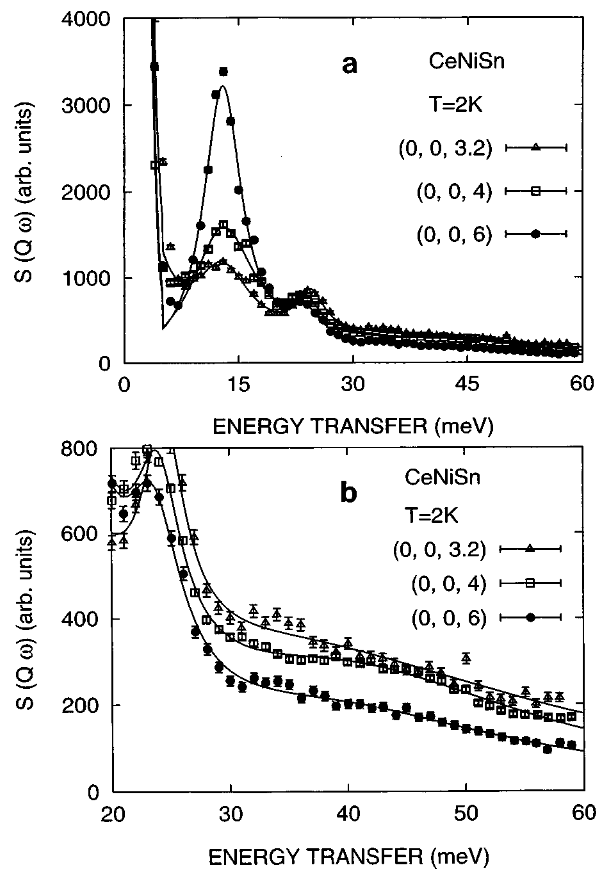


FIG. 2. (a) Inelastic spectra for $Q=(0,0,l)$ with $l=3.2$, 4, and 6. The solid lines are fits using the parameters of Table I. The high-energy results are shown enlarged in (b).

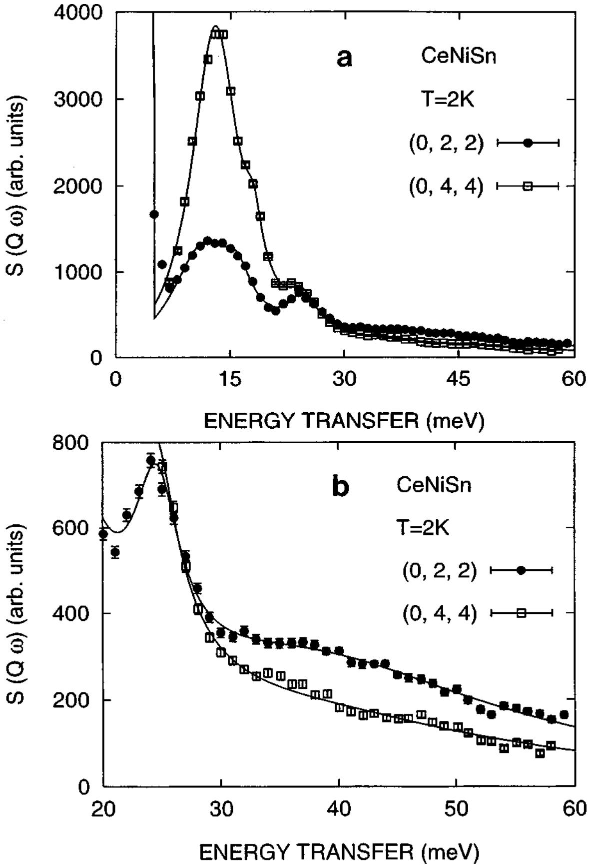


FIG. 3. (a) and (b) Inelastic spectra for $Q=(0,2,2)$ and $(0,4,4)$ with fitted curves as described previously.

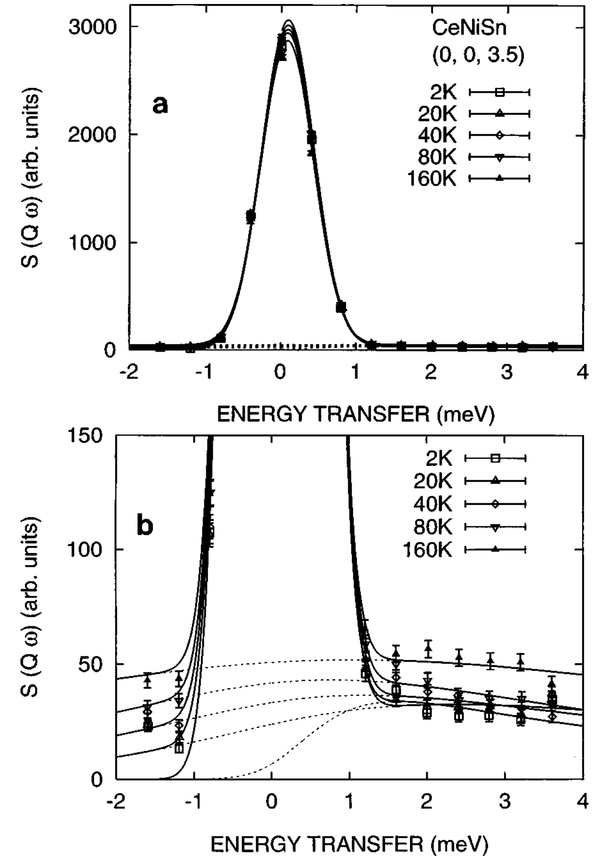


FIG. 4. Temperature dependence of the quasielastic neutron scattering at $Q=(0,0,3.5)$ between $T=2$ K and 160 K shown in full (a) and enlarged (b). Dashed lines represent fits of the quasielastic contribution alone; the solid line shows the results of fitting each scan to both quasielastic and nuclear contributions.

perature dependence of its linewidth, i.e., the low-lying excitations. In this temperature range, we observed a weak quasielastic-type contribution (see Fig. 4). Although this contribution is indeed very weak, it is nevertheless clear from the data as the scattering increases with temperature. This suggests that it is not of nuclear origin. However, the presence of a small phonon contribution at high temperatures cannot be ruled out completely at the moment. We have attempted to estimate the linewidth of the quasielastic scattering using a Lorentzian line shape convoluted with the Gaussian instrumental resolution function: the intrinsic quasielastic linewidth at 2 K is 1.6 meV. This value agrees well with that observed previously in polycrystal CeNiSn (1.6–1.9 meV).[7] Within the experimental accuracy, our results are consistent with the square-root temperature behavior of heavy-fermion compounds.[8] However, this needs to be confirmed with more detailed studies at higher resolution.

## IV. DISCUSSION

As we have shown, the 40-meV excitation is undoubtedly due to a crystal-field excitation on the $Ce^{3+}$ ions. This conclusion is supported by the fact that the intensity is reduced with increasing wave vector, while it is present in all the scans, i.e., it is a single-ion response. Since Ce in CeNiSn is at a site of lower than cubic symmetry, it is expected that the Ce $4f^1$ state of CeNiSn will be split into three doublets. In fact, CePtSn, which has the same $\varepsilon$-TiNiSn structure as CeNiSn, shows two clear magnetic excitations at 24 and 35 meV, respectively.[7]

Then why do we observe only one magnetic excitation in CeNiSn in our inelastic-neutron-scattering data? To answer this question, we need to examine again the data for polycrystalline Ce(Pt,Ni)Sn. The two magnetic excitations seen in CePtSn become weaker and broader with increasing Ni doping, which indicates that the hybridization between the Ce $4f$ electrons and the conduction electrons becomes stronger for $Ce(Pt_{1-x}Ni_x)Sn$. This interpretation that the behavior of the Ce $4f$ crystal-field excitations with increasing Ni concentration is due to the effects of strengthening hybridization with the conduction electrons is also in good agreement with the bulk property measurements:[9] CePtSn has an antiferromagnetic ground state with $T_N=7.5$ K and with Ni doping Ce(Pt,Ni)Sn becomes paramagnetic. As the previous polycrystalline data[7] and our results show, CeNiSn seems to have only the higher excitation, and not the lower energy excitation found in CePtSn.

Regarding the other excitation seen at 24 meV for CePtSn, we should note that with increasing Ni concentrations, not only do the peaks become broadened, but also the 24-meV excitation is suppressed more rapidly than the 35-meV excitation: we believe that the structure at 35 meV in the polycrystalline data is what we observe around 40 meV in our single-crystal results. This may indicate a different hybridization effect for the 24- and 35-meV excitations. It is not easy to determine whether we have lost completely the 24-meV excitation in pure CeNiSn, because of the phonon peak at almost the same energy.

In any case, whatever happens to the 24-meV magnetic excitation with Ni doping in CePtSn, it is clear that it is preferentially more quenched than the 35-meV structure because of the stronger hybridization between this $4f$ crystal-field state and the conduction electrons.

We now consider the implications of our results on the understanding of the CeNiSn ground state. First of all, our data show one crystal-field excitation beyond doubt, and with the help of the previous polycrystal Ce(Pt,Ni)Sn data we can deduce the rapid quenching of the other one at 24 meV in pure CeNiSn. Therefore it is likely that there is no other crystal-field excitations present at an energy lower than the Kondo energy of 80 K for interactions with the conduction electrons. This then means that a scenario put forward in Ref. 6 for the low-temperature and low-energy features in neutron scattering of CeNiSn cannot be true, since CeNiSn cannot possibly have such a low-energy crystal-field excitation.

In order to elucidate further the question of the 24-meV magnetic excitations in CeNiSn, we plan to examine this energy range with polarized neutrons to avoid the difficulties due to the phonon structure at nearby energies.

## ACKNOWLEDGMENTS

This research was supported at Inha University by the Ministry of Education, Korea (Grant No. KRA-96-04-D-0206) and the ICNSRF; at Southampton University, Birkbeck College, and the University of Birmingham by the UK Engineering and Physical Sciences Research Council.

*Present address: Department of Physics and Astronomy, University College London, Gower Street, London WC1E 6BT, UK.

[1] T. Takabatake, F. Teshima, H. Fujii, S. Nishigori, T. Suzuki, T. Fujita, Y. Yamaguchi, J. Sakurai, and D. Jaccard, Phys. Rev. B **41**, 9607 (1990); **45**, 5740 (1992).

[2] M. Kyogaku, Y. Kitaoka, K. Asayama, T. Takabatake, and H. Fujii, J. Phys. Soc. Jpn. **61**, 43 (1992).

[3] T. Takabatake, M. Nagasawa, H. Fujii, M. Nohara, T. Suzuki, T. Fujita, G. Kido, and T. Hiraoka, J. Magn. Magn. Mater. **108**, 155 (1992).

[4] T. Takabatake, G. Nakamoto, T. Yoshino, H. Fujii, K. Izawa, S. Nishigori, H. Goshima, T. Suzuki, T. Fujita, K. Maezawa, T. Hiraoka, Y. Okayama, I. Oguro, A. A. Menovsky, K. Neumaier, A. Bruckl, and K. Andres, Physica B **223&224**, 413 (1996).

[5] T. E. Mason, G. Aeppli, A. P. Ramirez, K. N. Clausen, C. Broholm, N. Stucheli, E. Bucher, and T. T. M. Palstra, Phys. Rev. Lett. **69**, 490 (1992); T. J. Sato, H. Kadowaki, H. Yoshizawa, T. Ekino, T. Takabatake, H. Fujii, L. P. Regnault, and Y. Isikawa, J. Phys.: Condens. Matter **7**, 8009 (1995).

[6] K. A. Kikoin, A. de Visser, K. Bakker, and T. Takabatake, Z. Phys. B **94**, 79 (1994); Yu. Kagan, K. A. Kikoin, and N. V. Prokofev, Physica B **199&200**, 211 (1994); **230-232**, 680 (1997); Yu Kagan, K. A. Kikoin, and A. S. Mishchenko, Phys. Rev. B **55**, 12 348 (1997).

[7] D. T. Adroja, B. D. Rainford, A. J. Neville, and A. G. M. Jansen, Physica B **223&224**, 275 (1996).

[8] E. Holland-Moritz and G. H. Lander, in *Handbook on the Physics and Chemistry of Rare Earths* (Elsevier, Amsterdam, 1994), Vol. 19.

[9] J. Sakurai, R. Kawamura, T. Taniguchi, S. Nishigori, S. Ikeda, H. Goshima, T. Suzuki, and T. Fujita, J. Magn. Magn. Mater. **104-107**, 1415 (1992).